On the Magnitude of the Electric Field near Thunderstorm-Associated Clouds

FRANCIS J. MERCERET AND JENNIFER G. WARD

National Aeronautics and Space Administration, Kennedy Space Center, Florida

DOUGLAS M. MACH

University of Alabama in Huntsville, Huntsville, Alabama

MONTE G. BATEMAN

Universities Space Research Association, Huntsville, Alabama

JAMES E. DYE

National Center for Atmospheric Research, Boulder, Colorado*

(Manuscript received 6 February 2007, in final form 9 May 2007)

ABSTRACT

Electric-field measurements made in and near clouds during two airborne field programs are presented. Aircraft equipped with multiple electric-field mills and cloud physics sensors were flown near active convection and into thunderstorm anvil and debris clouds. The magnitude of the electric field was measured as a function of position with respect to the cloud edge to provide an observational basis for modifications to the lightning launch commit criteria (LLCC) used by the U.S. space program. These LLCC are used to reduce the risk that an ascending launch vehicle will trigger a lightning strike that could cause the loss of the mission or vehicle. Even with fields of tens of kV m^{-1} inside electrically active convective clouds, the fields external to these clouds decay to less than 3 kV m^{-1} within 15 km of cloud edge. Fields that exceed 3 kV m^{-1} were not found external to anvil and debris clouds.

1. Introduction

This paper presents measurements of electric fields aloft in and near clouds associated with thunderstorms. The emphasis is on thunderstorm anvil and debris clouds associated with the decaying phase of thunderstorms. An excellent summary of published measurements of thunderstorm electric fields aloft through the mid-1990s may be found in chapter 7 of MacGorman and Rust (1998). Nearly all of those measurements were made in cloud, and most were taken during the growth or mature stage of the storms.

Electric fields in or near anvils and debris clouds are of concern to aviation and aerospace interests because of the threat of triggered lightning. Air- and spacecraft completely avoid flight through active convection because of the multiple threats of natural and triggered lightning, wind shear, turbulence, and hail. Anvils and debris clouds produced by thunderstorms cover much more airspace and can persist longer than the convective cores that produce them. Unconditional avoidance of all such clouds would unnecessarily cause delays or diversions of air traffic and delays or scrubs of aerospace launch and landing operations. However, even in the absence of natural lightning, lightning may be triggered in or near such clouds if the electric fields are high enough. Triggered lightning has destroyed both aircraft and space vehicles. An excellent summary of the matter is found in chapter 10 of Rakov and Uman (2003).

For space launches, the National Aeronautics and Space Administration (NASA) and the U.S. Air Force

* The National Center for Atmospheric Research is sponsored by the National Science Foundation.

Corresponding author address: Francis J. Merceret, NASA/KT-C-H, Kennedy Space Center, FL 32899.
E-mail: francis.j.merceret@nasa.gov

DOI: 10.1175/2007JAMC1713.1

developed a set of lightning launch commit criteria (LLCC) to protect vehicles from natural and triggered lightning during ascent. These LLCC prohibit flight through or close to specific types of clouds, including anvil and debris clouds, depending on the optical and radar properties of the clouds and the time of occurrence of the last lightning in the cloud or its parent thunderstorm. Specific standoff distances and waiting times are provided. Details may be found in Willett et al. (1999). These rules are safe but can be very restrictive. In the early 1990s, NASA conducted an airborne field mill (ABFM) program (hereinafter referred to as ABFM-I) to measure electric fields aloft in and near thunderstorm-related clouds to determine whether the LLCC could be safely relaxed. A second ABFM program, ABFM-II, was conducted during 2000 and 2001. The two programs were similar overall, but the objectives differed significantly. ABFM-I is described in Christian et al. (1993). ABFM-II is described in Merceret and Christian (2000) and Dye et al. (2004, 2007).

This paper presents the results of one aspect of these ABFM efforts: the decrease in magnitude of the electric field with distance from cloud edge. If it could be shown that the electric field, which may be tens or even hundreds of kV m^{-1} in cloud, becomes small (<3 kV m^{-1}) at a short distance outside the cloud, then the standoff distances in the current LLCCs may be safely reduced. The threshold of 3 kV m^{-1} is thought to be sufficient to protect against the threat of rocket-triggered lightning based on the typical length of ionized rocket plumes. Electric fields below the threshold should not produce a high enough potential across the length of the rocket and its plume to sustain a lightning discharge. Section 2 of the paper describes ABFM-I and its results. Section 3 describes ABFM-II and its results. Section 4 discusses the common findings, differences, and implications of the two programs.

2. ABFM-I

a. Description

The ABFM-I program consisted of four deployments to the Kennedy Space Center (KSC) area, with two deployments during summer and two during winter conditions found in Florida near KSC. The summer goals included determining when developing cumulus become a hazard to launch vehicles, how far away from mature clouds the hazardous fields extend, and when the thunderstorm debris clouds are no longer a hazard to launch vehicles. The main winter target was layered clouds. The winter goals included determining at what overall thickness layered clouds (including but not limited to altostratus and cirrostratus) become a hazard to launch vehicles and whether there were other measurements of how to determine if a layered cloud was, or was not, a hazard. In addition, all deployments were used to test the ability of a network of 31 ground-based field mills (GBFM) at KSC and Cape Canaveral Air Force Station to detect electrically hazardous conditions aloft. The first summer deployment was in July and August 1990 and consisted of 31 data flights. The first winter deployment was in February and March 1991 and had 18 data flights. The second summer deployment was in July and August 1991 and also had 31 data flights. The second winter deployment was in January–March 1992 and had 25 data flights.

The ABFM-I data presented in this paper were collected in the vicinity of vigorously growing cumulus or thunderstorms. One of the consequences is that the "screening layer" that can form at cloud boundaries is expected to be absent or only weakly present in the ABFM-I target clouds. Charge in the interior of a cloud attracts charge of the opposite sign from the surrounding air. At the cloud boundary, the relatively high conductivity of the clear air gives way to the lower conductivity of the cloudy air. Thus, the attracted charge tends to accumulate at the edges of the cloud. If the cloud is growing, that charge layer gets entrained into the cloud and diluted or neutralized. Vonnegut et al. (1966) present measurements demonstrating this at the upper cloud boundary. In addition, because the clouds in ABFM-I were at the beginning of their life cycle, the screening layers did not have much time to form.

In contrast, the data collected during ABFM-II, described in section 3, were from decaying thunderstorm anvils or debris clouds. If the cloud is not growing, the attracted charge accumulates on the boundary of the cloud, shielding the fields within the cloud. Outside of the cloud, the field caused by this screening layer tends to cancel the field caused by the charge in the cloud interior. That may be one reason why the data show stronger fields outside of the clouds in ABFM-I than in ABFM-II, although further research is clearly required because the evidence for horizontal screening layers is weak at best (Dye et al. 2007).

For ABFM-I, target clouds were first identified with radar. If the target was a growing cumulus, the aircraft was then directed to fly at the top of the growing cloud (just penetrating the top edge of the cloud). If the target was a mature cumulus, the aircraft was directed to fly toward the cloud and then turn away either at the edge or farther out from the cloud (depending on the severity of the target). In all cases, the aircraft was to avoid areas with known lightning or reflectivity values of 30 dBZ or more based on returns from the onboard radar.

b. Instrumentation

The aircraft used was a Learjet 28/29 (experimental hybrid) business jet, operated by NASA Langley Research Center. The aircraft carried five rotating-vane-type electric-field mills and a data collection system consisting of an IBM Corporation PC-AT personal computer with an Exabyte tape recorder. The data were also telemetered to ground and recorded there.

The Learjet 28/29 carried a liquid water content (LWC) King probe, made by Particle Measurement Systems, Inc. (PMS). It also had a "charging patch" (Davis et al. 1989) that sensed the presence of ice crystals by differential charging. Combining these two gave indications that the aircraft was flying in liquid, mixed-phase, or ice clouds. In addition, pilots were given the task of noting entry into and exit from cloud as accurately as possible. The charging patch was used to distinguish ice clouds from those without ice.

Volume scan reflectivity data were available from the Weather Surveillance Radar (WSR-74C) located at Patrick Air Force Base, Florida. This radar is a C-band (5.3 cm) horizontally polarized conventional weather radar. Because of calibration issues during ABFM-I, this radar could not be used quantitatively to relate measured electric fields to radar reflectivity. Despite the calibration uncertainties, the measured values are believed to be close to the true values. Thus, it was useful for characterizing the general environment in which the data were taken.

There was also a small lightning ground-strike location system installed at KSC, and it was used to warn the pilots away from storms with lightning. A more detailed description of all of the instrumentation for ABFM-I may be found in Fisher et al. (1992).

c. Data analysis

The five field mills on the aircraft were first calibrated in the laboratory to determine the basic instrument calibration constant that converts output voltage to electric field. Once the mills were mounted on the aircraft, the aircraft was directed to perform a series of roll and pitch maneuvers at low altitude under fair-weather conditions. Because the fair-weather field is vertical and is reasonably known, the roll and pitch maneuvers rotated the predominantly vertical field (Ez) into the other components (Ex and Ey). By manually examining the various mill responses to the roll and pitch maneuvers, a relative calibration relationship (or matrix) between the mill outputs and the external electric field was determined. A high-voltage "stinger" was used to charge the aircraft to determine the final relative calibration. A series of flybys of a calibrated ground-based field mill provided the final absolute calibration. See Mach and Koshak (2007) for details of the full calibration process.

The data were monitored in real time on the ground and on the aircraft. Each field mill produced a periodic calibration pulse used to monitor the health and calibration of the field mill. Any problems with the mills or the calibrations were noted in the datalogs. The real-time telemetered data were recorded on the ground on Exabyte tapes, and the data recorded on the aircraft were transferred to Exabyte tape in the same format for archiving.

During ABFM-I, the cloud edge was determined manually using three methods: 1) pilot report (visually), 2) the outer edge of the 2-dBZ radar echo, and 3) LWC probe or charge patch. The 2-dBZ threshold was selected because it agreed with the visual cloud edge when a visual edge was observed. The mean and standard deviation of the magnitude of the electric field outside of the cloud were determined as a function of distance from cloud edge. No attempt was made to determine the variation of the fields inside the cloud as a function of cloud-edge distance.

d. Results for developing cumuli

For ABFM-I, 43 developing cumuli were sampled in 1990 and 44 were sampled in 1991. The results indicated that the observed electric fields depended strongly on the cloud-top height as defined by the uncalibrated 10-dBZ reflectivity. Fields in clouds with 10-dBZ tops lower than the 0°C level did not exceed 3 kV m^{-1}.

Clouds with tops between 0° and −10°C sometimes had fields greater than 1 kV m^{-1}. There were 3 cases in which a cloud was very near the −10°C level and growing rapidly that had fields greater than 3 (but less than 5) kV m^{-1}. However, the vast majority of the clouds in this altitude range had fields less than 1 kV m^{-1}.

Fields greater than 3–5 kV m^{-1} did not develop in the clouds until the echo top of the cloud had grown higher than the −10°C level (average altitude 6.4 km above mean sea level). Furthermore, the study clouds did not produce lightning until the tops were higher than the −20°C level. Fields at the edge of clouds with echo tops higher than the −20°C level could be greater than 50 kV m^{-1}.

Figure 1 shows the average and peak electric-field magnitudes for ABFM-I approaches to active convection as a function of distance from cloud edge. If the cloud was not penetrated by the aircraft (because of lightning or excessive fields), the uncalibrated 2-dBZ echo edge was used as the cloud boundary. Some of these clouds were associated with storms that were producing lightning at the time the measurements were

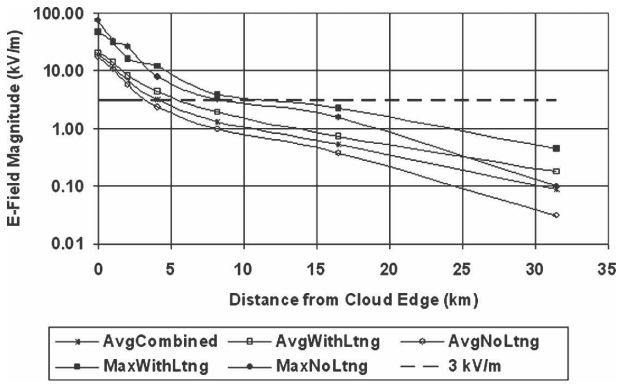

FIG. 1. Electric-field magnitude for ABFM-I as a function of distance from the edge of actively growing storms. In the legend, "Avg" denotes the average and "Max" denotes the peak magnitude of the field. "WithLtng" denotes storms with active lightning, and "NoLtng" denotes those without active lightning at the time of sampling. The "Combined" curve includes all storms without regard for the presence of active lightning at the time of sampling.

taken. Penetrations with and without lightning were averaged both separately and combined. Peak values are shown only for the separate cases because the combined case is merely the maximum of the separate cases.

For these actively growing storms, the magnitude of the electric field was reliably below the 3 kV m^{-1} threshold for distances larger than 15 km. Even in clouds with tops above −20°C, the maximum fields dropped off to less than 3 kV m^{-1} by 8 km from the edge of the cloud in the absence of lightning. In most cases, the fields decayed much more quickly than these values. The average value was below the threshold beyond 6 km even for storms actively producing lightning.

3. ABFM-II

a. Description

The ABFM-II campaigns were conducted during June 2000 and May–June 2001 to obtain ground-based radar measurements simultaneously with airborne measurements of the electric fields and microphysical content in anvil clouds, thick clouds, and debris clouds near Kennedy Space Center. Flights of the University of North Dakota Citation II jet aircraft were coordinated with the WSR-74C 5-cm radar at Patrick Air Force Base, which was well calibrated for ABFM-II, and the 10-cm Weather Surveillance Radar-1988 Doppler (WSR-88D) at Melbourne, Florida. When possible, flights were conducted over the GBFM network at KSC and in the operating range of the KSC Lightning Detection and Ranging (LDAR) system and the Cloud-to-Ground Lightning Surveillance System (CGLSS).

During the campaign, initial anvil penetrations were typically made near to and somewhat downstream from the convective cores of storms in the mature to decaying stage. Subsequent passes were made across the anvil at different distances downstream to examine the decay of the electric field both with time and distance. Anvils were sampled during 19 flights at a wide variety of altitudes in different locations relative to anvil top and bottom and relative to distance from the storm core. There is enough variety in these measurements to be representative of conditions in anvils of Florida thunderstorms. Various flight plans were used to sample the cloud as a function of distance (which corresponds to translation time) from the core. Some flights were made across the anvil, with each subsequent pass at a higher or lower altitude in stairstep fashion. Some flights were made along the downwind axis of the anvil to measure electric field versus the translation time (i.e., time for electric field to decay) at different positions in the downwind anvil. Some flights were made after convection in the core had ceased and the anvil was dissipating but while enhanced electric fields still existed. Decisions on where to fly were interactive between crew in the aircraft and aircraft coordinators at the Range Operations Control Center.

A critical measurement from the aircraft was the in situ measurement of the three-dimensional electric field. This was accomplished using six high-sensitivity, low-noise electric-field mills described in section 3b below. The microphysical observations were made with several different instruments also described in section 3b. Information on the operating characteristics of the University of North Dakota Citation II jet aircraft and the instruments flown during ABFM-II can be found in the appendixes of Dye et al. (2004) and in Dye et al. (2007). The Citation II had an operating ceiling of 13.1 km. It could cruise at speeds of up to 175 m s^{-1} and climb at 16.8 m s^{-1} with an on-station time of up to 4 h depending on mission type. It could safely be flown at speeds as low as 72 m s^{-1} when necessary for some kinds of measurements.

b. Instrumentation

The rotating-vane field mills flown during ABFM-II were designed and built by the NASA Marshall Space Flight Center. These mills are described in detail in Bateman et al. (2007). Six mills were used to ensure adequate data to resolve the vector components of the field plus the field due to charge on the aircraft and to ensure some redundancy for data quality control. The data collection system was a Pentium-class personal computer. A GPS card was used to keep the data time

synchronized to UTC. The computer synchronizes the data collection for each mill and also records the data that the mill sends back. The field data were displayed and used in real time along with radar to advise the pilot on safety.

ABFM-II used volume-scan reflectivity data from the same WSR-74C weather radar located at Patrick Air Force Base that was used for ABFM-I. However, for ABFM-II this radar was calibrated to within ±1 dBZ and could be used quantitatively. In addition, ABFM-II also used level-2 volume-scan reflectivity data from the WSR-88D Next Generation Weather Radar (NEXRAD) at Melbourne (KMLB). Comparisons of measurements from the two radars for a few times and storms showed agreement to within 2–3 dBZ when attenuation of the 5-cm WSR-74C was not an issue.

ABFM-II used lightning location information from two sources: the LDAR operated by NASA at KSC and CGLSS operated by the U.S. Air Force at their Eastern Range. CGLSS provides the location of the return strokes of cloud-to-ground lightning with an accuracy such that 50% are located within 300 m of their actual position when that position is within 40 km of the center of the network near KSC. The accuracy degrades to 3 km at a distance of 100 km. The detection efficiency for flashes is greater than 90%. LDAR locates the three-dimensional path of each flash with an accuracy of 100 m within 10 km of the center of the network at KSC and with an accuracy of 1 km to a range of 100 km. The detection efficiency exceeds 90%. The advantage of LDAR is that it locates in-cloud lightning as well as cloud-to-ground lightning. Additional information on both systems may be found in Maier et al. (1995). As with ABFM-I, lightning data were used for flight safety. They were also used during analysis to determine the time and distance of the last lightning flash either in the cloud being penetrated or one nearby.

During ABFM-II, particle measurements were made with five different particle probes that spanned particle sizes from a few micrometers to about 5 cm and thus from frozen cloud droplets to very large aggregates. To determine cloud edge, the primary microphysical instruments were the PMS Optical Array 2D Cloud (2D-C) probe with a range from ~30 μm to a few millimeters [see Strapp et al. (2001) for a recent discussion of the 2D-C probe], the PMS Optical Array 1D Cloud (1D-C) probe with a range from 20 to 600 μm, and the PMS Forward Scattering Spectrometer Probe (FSSP) with a range for water droplets from ~3 to 50 μm (Dye and Baumgardner 1984). Although the community has used the FSSP primarily for the measurement of cloud droplets it is also effective at detecting ice particles, but sizing is inaccurate and the measured concentrations are overestimates as a result of particles shattering on the probe tips, especially in broad ice particle spectra such as those we found in Florida anvils [see Field et al. (2003) for a discussion of this problem]. It was not a primary instrument for detecting cloud edge in this study because spurious counts often appeared in the smaller size bins, even out of cloud.

Each of the particle instruments was calibrated using standard calibration techniques. The measurements from these probes were processed and displayed using software developed at the National Center for Atmospheric Research. Data from each of these sensors were processed to produce size distributions for each probe averaged over 10-s time periods. The agreement between the 1D-C and the 2D-C in the region of overlap was in general very good except for the smallest sizes, where the instrument response was an issue, and the largest sizes, where the sample sizes are small (Dye et al. 2007). In most circumstances the entries into or exits from cloud determined from the individual instruments agreed very well.

c. Data analysis

Analysis of ABFM-II data was based on composite files created for each flight by merging measurements from airborne, surface, and radar sources. The instruments used to make these measurements were carefully calibrated and quality controlled. These merged files contained 10-s averages of time-synchronized aircraft measurements, including electric fields and particle measurements with the corresponding radar reflectivity measurement for the location and altitude of the aircraft at that time. For the nominal speed of the aircraft of 120 m s^{-1}, 10 s corresponds to approximately 1.2 km of flight track and is roughly equivalent to the 1-km gridding of the radar data. These merged files contained radar observations from both WSR-74C and NEXRAD WSR-88D. An example of a graphical display showing both radar and airborne measurements generated from a merged dataset is presented in Fig. 2.

The merged data files were used extensively for a number of different studies over a 2-yr period following the field campaigns. During the analysis, an occasional timing error or other problem became apparent. As problems were found, corrections were made to the dataset and files. This dataset is now mature, of high quality, and unlikely to contain errors that would have an impact on this study. It is archived online (http://abfm.ksc.nasa.gov).

For the results presented in this paper we have in-

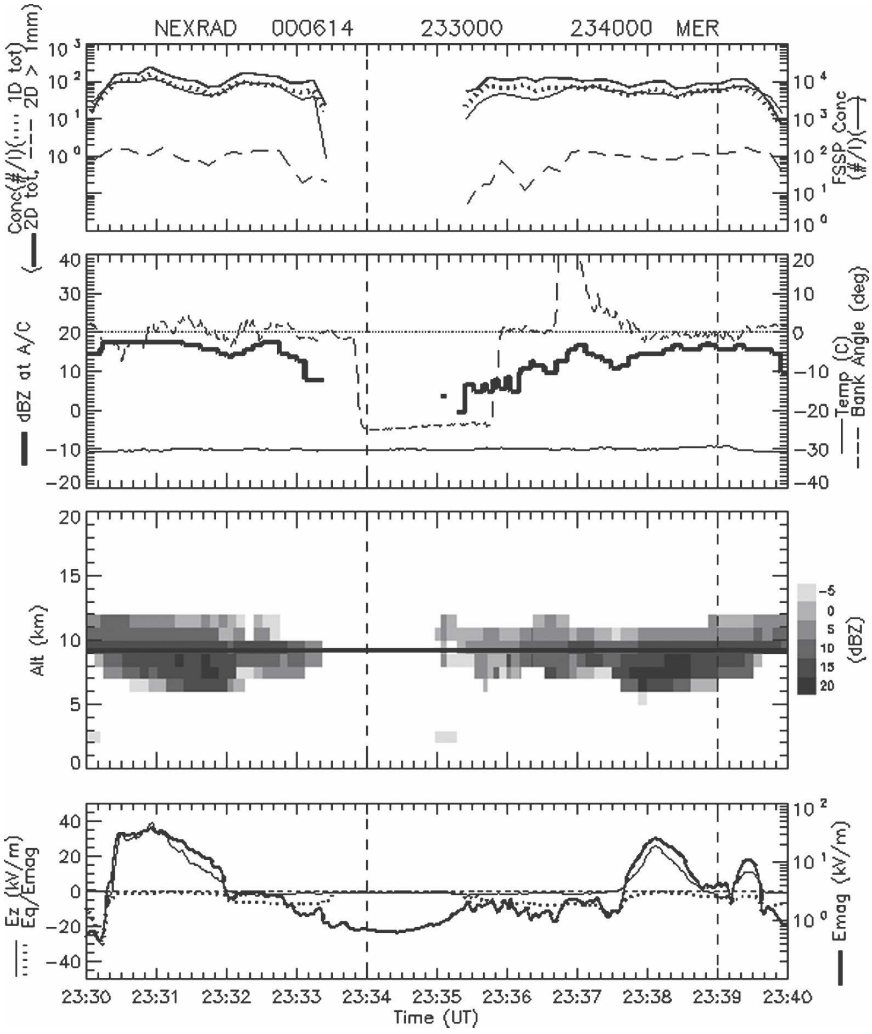

FIG. 2. Typical MER plot. (top) Cloud particle concentrations from the 1D-C, 2D-C, and FSSP instruments. (upper middle) Ground-based radar reflectivity along with the air temperature at the aircraft position plus the aircraft bank angle. (lower middle) A time–height presentation of ground-based radar reflectivity in a plane containing the aircraft track from the ground to the top of the radar scan. The thick line is the aircraft track. (bottom) Electric-field components measured at the aircraft. The thick line is the scalar magnitude, the thin line is the vertical component, and the dotted line is the field due to charge on the aircraft divided by the magnitude of the ambient field.

cluded only those measurements that were made in close proximity to or inside anvils or debris clouds. To be considered an anvil for this analysis, a cloud must have had the morphological structure of an anvil (i.e., it was produced by a downshear or upshear outflow or blow-off from an active cumulus convective core and it had a well-defined base). The convective core may either still exist at the time of the penetration or could have decayed (i.e., the anvil can be attached or detached). This requires determining the previous history of the cloud in question using a sequence of radar images. Decay products left in place at higher altitudes from once active convective cores growing in a low-shear environment are *not* considered to be an anvil, but for the purpose of this paper they are referred to as debris clouds.

In contrast to the strategy and results obtained from ABFM-I, where the focus tended to be on the core of developing cumuli or on approaching the cloud edge of the core of active mature storms, the emphasis in ABFM-II was on measurements in anvils and debris clouds mostly away from storm cores. The flight strategies and subsequent data classification of ABFM-I and ABFM-II were very different. As a consequence, the

results obtained from the two projects were also different. There are similarities in that the electric fields fall off rapidly from cloud edge for both datasets, but the magnitude of the field is larger near the growing and active clouds of ABFM-I.

Because of the large amount of data and the tediousness of manual analysis, the distance from cloud edge for ABFM-II was computed automatically. The position of the cloud edge was determined using the algorithm described by Ward and Merceret (2004). It determines whether the aircraft is in or out of cloud based primarily on 2D-C cloud particle measurements or, under certain conditions, 1D-C measurements and radar data. Cloud edges are determined from transitions between being in and out of cloud, subject to a hysteresis constraint.

The distance from the identified cloud edge was computed based on the aircraft speed and three assumptions about the flight track. The aircraft flew at a nominal speed of 120 m s^{-1} and so each 10-s record was assumed to represent 1.2 km of travel horizontally. The other assumptions were that the flight track was essentially perpendicular to the cloud edge and that there were no underlying or overhanging clouds closer to the aircraft than the computed horizontal distance from the cloud. The perpendicularity assumption was generally valid because the flight tracks were selected to transect the cloud across or along its major axis. The assumption about clouds overhanging or underlying the aircraft was frequently invalid, and these cases had to be detected and eliminated as described in the next paragraph.

The automated algorithm provided a list of the date and time of each cloud entry and exit it detected. The radar cross sections along the flight track, such as the example shown in the microphysics, electric field, and radar (MER) plot in Fig. 2, were examined for each case to ensure that the assumption discussed above was valid. Entries or exits with significant underlying or overhanging cloud were eliminated from the analysis since the distances from cloud edge generated in the statistical database were invalid. A typical example of an invalid entry is shown in Fig. 3. Here the aircraft flew less than 1 km below cloud base but outside of the cloud as determined by both cloud physics and radar data for 50 s before entering the cloud. The fields measured during those 50 s would be reported as fields at distances ranging from 1 to 6 km rather than at their actual distance if this case were kept in the database.

For the ABFM-II data, the maximum, mean, and other statistics of the electric-field magnitude were computed as a function of distance from cloud edge. Anvil and debris cloud were treated separately to determine whether the results significantly differed. Because only fields of 3 kV m^{-1} or greater were considered to be hazardous for our purposes, the analysis excluded cases in which the maximum field magnitude within the cloud was less than that value. The inclusion of fields associated with nonhazardous clouds would reduce the average and median values, thus providing a false indication of the actual threat in the vicinity of strongly electrified clouds.

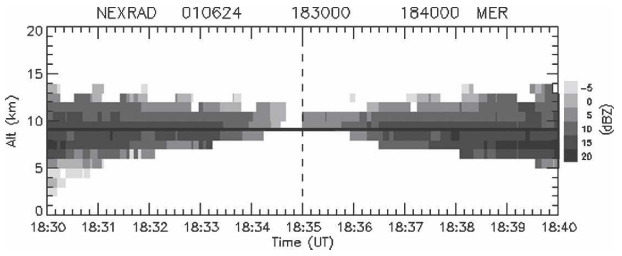

FIG. 3. Radar panel of MER plot at 1830–1840 UTC 24 Jun 2001, showing a vertical cross section of the reflectivity (dBZ) along the aircraft flight track. Data are from the KMLB WSR-88D (NEXRAD). The vertical axis is altitude (km). The horizontal axis is time (UTC): each major tick represents 1 min. The aircraft position is given by the solid black line near 9-km altitude. It entered the anvil nearly one major tick to the right of center at 1835:50 but was flying less than 1 km below cloud base beginning at 1835:00 at the center of the figure.

d. Results

Maximum and average values of the magnitude of the electric field as a function of distance from cloud edge are shown for anvils and debris clouds, respectively, in Figs. 4 and 5. These are based on penetrations of 18 anvil clouds and 11 debris clouds. The statistical sampling error in Fig. 2 is 120 V m^{-1} from the cloud edge outward and rises to a maximum of 3.8 kV m^{-1} in the high-field portion of the interior of the cloud. The corresponding sampling errors for Fig. 5 are 182 V m^{-1} and 6.5 kV m^{-1}. The behavior is very similar. The field magnitudes drop below the hazard threshold of 3 kV m^{-1} inside the cloud before the edge is reached in both anvil and debris clouds even in the worst case. Fields below this threshold are believed not to pose a threat that a launch vehicle will trigger lightning (Willett et al. 1999). The average fields outside the cloud do not exceed 1 kV m^{-1} right up to cloud edge.

The figures also show that the debris clouds had generally larger fields than did anvils in the cloud interiors, but, from the cloud edge outward, the fields near anvil and debris clouds behaved almost identically. This result suggests that in determining safe external standoff distances for LLCC, anvil and debris clouds may be treated in the same manner.

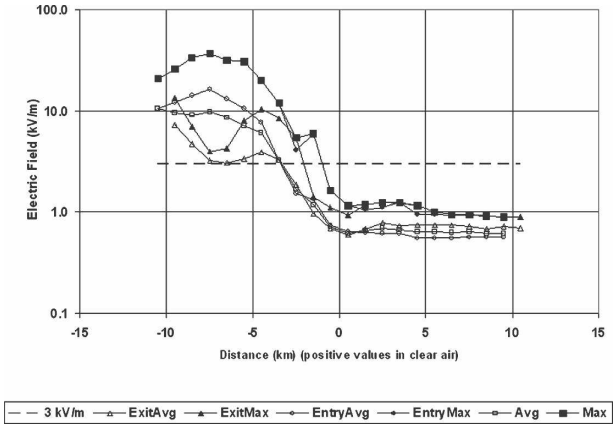

FIG. 4. Electric-field magnitude as a function of distance from the edge of anvil clouds in ABFM-II having a maximum field magnitude of at least 3 kV m^{-1}. The maximum and average values are shown separately for passes entering cloud and exiting cloud. The hazard threshold of 3 kV m^{-1} is shown by a horizontal dashed line. The cloud boundary is at the midpoint of the chart (distance = 0) with cloud on the left and clear air on the right.

4. Discussion

In contrast with the ABFM-I results in clouds associated with active storms exhibiting charge production and lightning, the maximum fields measured during ABFM-II fell below hazardous levels everywhere outside of the cloud, even when the fields several kilometers inside the cloud were tens of thousands of volts per meter. Figure 6 presents the average and peak field magnitudes for both experiments as a function of distance from the cloud edge. The ABFM-II anvil and debris data are combined in this figure because they are so similar. To combine the data in the most conservative (safe) way from the point of view of application to LLCC development, at each distance, the larger of the anvil or debris statistics was plotted for comparison with ABFM-I. The ABFM-I maximum data in the figure were not dominated by a single case. Of 60 cases, 16 had high fields at cloud edge.

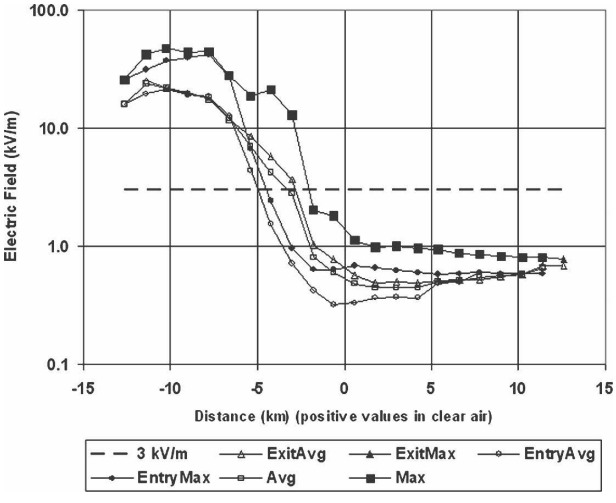

FIG. 5. As in Fig. 4, but for debris cloud.

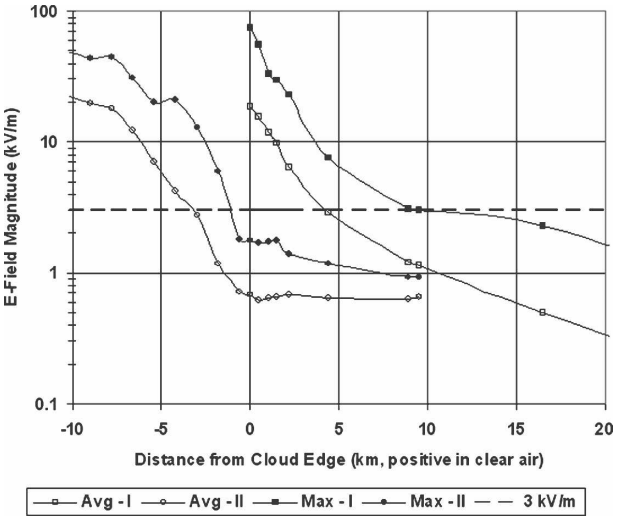

FIG. 6. Comparison of the average and maximum electric fields measured by ABFM-I and ABFM-II as a function of distance from cloud edge. Positive distances are outside the cloud, and negative distances are within the cloud. ABFM-I did not measure fields inside the cloud and only studied active cumulus clouds. For the ABFM-II statistics, the average and maximum shown here are the larger, respectively, of the average or maximum of either anvil or debris cloud at each distance.

The data suggest that cumulus clouds associated with active, charge-producing thunderstorms may produce external electric fields that exceed 3 kV m^{-1} up to as much as 15 km from cloud edge. Conversely, when only anvil or debris clouds are considered, the external field magnitude is benign right up to the cloud edge even with large fields in the cloud interior.

The observations reported here may permit some relaxation of the standoff distances in the operational LLCC for anvils of the type penetrated in ABFM-II. Depending on the rule, these distances are currently set at 9.26 km (5 n mi) or 18.52 km (10 n mi). If these distances could be reduced significantly with appropriate constraints for active storms, the number of unnecessary launch scrubs and delays resulting from violation of the LLCC could be proportionately reduced. The cost savings could be substantial at those launch sites where the threat of triggered lightning is a major concern. Before any such changes to the LLCC are approved, they will have to undergo a thorough risk analysis. The risk analysis must include examination of the representativeness of the clouds sampled in this experiment as well as the limited sample size.

Clouds of the type penetrated in ABFM-I, actively growing convective clouds, produce potentially hazardous fields at distances large enough to suggest that little if any reduction in the standoff distances in the LLCC may be advisable for these clouds.

Acknowledgments. The authors thank Tony Grainger and his team of scientists, engineers, and pilots at the University of North Dakota (UND) for their outstanding support with the UND Citation aircraft and instrumentation. We also thank Sharon Lewis and Mike Dye of the National Center for Atmospheric Research (NCAR) for creating and maintaining the NCAR data archive facility for the ABFM-II program. Funding for this project was provided by the National Aeronautics and Space Administration and the Department of Defense. Mention of a proprietary product or service does not constitute an endorsement thereof by the authors or their institutions.

REFERENCES

Bateman, M. G., M. F. Stewart, R. J. Blakeslee, S. J. Podgorny, H. J. Christian, D. M. Mach, J. C. Bailey, and D. Daskar, 2007: A low noise, microprocessor-controlled, internally digitizing rotating-vane electric field mill for airborne platforms. *J. Atmos. Oceanic Technol.,* **24,** 1245–1255.

Christian, H. J., D. M. Mach, and J. C. Bailey, 1993: The Airborne Field Mill Project: A program summary, A32E-03. *Eos, Trans. Amer. Geophys. Union,* **74** (Suppl.), 152.

Davis, R. E., D. V. Maddalon, R. D. Wagner, D. F. Fisher, and R. Young, 1989: Evaluation of cloud detection instruments and performance of laminar-flow leading-edge test articles during NASA leading-edge flight-test program. NASA Tech. Paper 2888, 62 pp. [Available from NASA Center for AeroSpace Information (CASI), 7121 Standard Drive, Hanover, MD 21076-1320.]

Dye, J. E., and D. Baumgardner, 1984: Evaluation of the forward scattering spectrometer probe. Part I: Electronic and optical studies. *J. Atmos. Oceanic Technol.,* **1,** 329–344.

——, S. Lewis, M. G. Bateman, D. M. Mach, F. J. Merceret, J. G. Ward, and C. A. Grainger, 2004: Final report on the Airborne Field Mill Project (ABFM) 2000–2001 field campaign. National Aeronautics and Space Administration Rep. NASA/TM-2004-211534, Kennedy Space Center, FL, 132 pp. [Available from NASA Center for AeroSpace Information (CASI), 7121 Standard Drive, Hanover, MD 21076-1320.]

——, and Coauthors, 2007: Electric fields, cloud microphysics and reflectivity in anvils of Florida thunderstorms. *J. Geophys. Res.,* **112,** D11215, doi:10.1029/2006JD007550.

Field, P. R., R. Wood, P. R. A. Brown, P. H. Kaye, E. Hirst, R. Greenaway, and J. A. Smith, 2003: Ice particle interarrival times measured with a fast FSSP. *J. Atmos. Oceanic Technol.,* **20,** 249–261.

Fisher, B. D., M. R. Phillips, and L. M. Maier, 1992: Joint NASA/USAF Airborne Field Mill Program—Operation and safety considerations during flights of a Lear 28 airplane in adverse weather. *Proc. Sixth Biennial Flight Test Conf.,* Hilton Head, SC, American Institute of Aeronautics and Astronautics, 1–16.

MacGorman, D. R., and W. D. Rust, 1998: *The Electrical Nature of Storms.* Oxford University Press, 422 pp.

Mach, D. M., and W. J. Koshak, 2007: General matrix inversion technique for the calibration of electric field sensor arrays on aircraft platforms. *J. Atmos. Oceanic Technol.,* **24,** 1576–1587.

Maier, M. W., L. M. Maier, and C. Lennon, 1995: Lightning detection and location systems for spacelift operations. Preprints, *Sixth Conf. on Aviation Weather Systems,* Dallas, TX, Amer. Meteor. Soc., 292–297.

Merceret, F. J., and H. Christian, 2000: KSC ABFM 2000—A field program to facilitate safe relaxation of the lightning launch commit criteria for America's space program. Preprints, *Ninth Conf. on Aviation, Range, and Aerospace Meteorology,* Orlando, FL, Amer. Meteor. Soc., 447–449.

Rakov, V. A., and M. A. Uman, 2003: *Lightning: Physics and Effects.* Cambridge University Press, 687 pp.

Strapp, J. W., F. Albers, A. Reuter, A. V. Korolev, U. Maixner, E. Rashke, and Z. Vukovic, 2001: Laboratory measurements of the response of a PMS OAP-2DC. *J. Atmos. Oceanic Technol.,* **18,** 1150–1170.

Vonnegut, B., C. B. Moore, R. P. Espinola, and H. H. Blau Jr., 1966: Electric potential gradients above thunderstorms. *J. Atmos. Sci.,* **23,** 764–770.

Ward, J. G., and F. J. Merceret, 2004: An automated cloud-edge detection algorithm using cloud physics and radar data. *J. Atmos. Oceanic Technol.,* **21,** 762–765.

Willett, J. C., H. C. Koons, E. P. Krider, R. L. Walterscheid, and W. D. Rust, 1999: Natural and triggered Lightning Launch Commit Criteria (LLCC). Aerospace Rep. A923563, Aerospace Corp., El Segundo, CA, 23 pp.